

Original Article

# Hypoxia/oxidative stress alters the pharmacokinetics of CPU86017-RS through mitochondrial dysfunction and NADPH oxidase activation

Jie GAO<sup>#</sup>, Xuan-sheng DING<sup>#</sup>, Yu-mao ZHANG<sup>#</sup>, De-zai DAI<sup>\*</sup>, Mei LIU, Can ZHANG, Yin DAI

Faculty of Pharmacy, China Pharmaceutical University, Nanjing 210009, China

**Aim:** Hypoxia/oxidative stress can alter the pharmacokinetics (PK) of CPU86017-RS, a novel antiarrhythmic agent. The aim of this study was to investigate the mechanisms underlying the alteration of PK of CPU86017-RS by hypoxia/oxidative stress.

**Methods:** Male SD rats exposed to normal or intermittent hypoxia (10% O<sub>2</sub>) were administered CPU86017-RS (20, 40 or 80 mg/kg, ig) for 8 consecutive days. The PK parameters of CPU86017-RS were examined on d 8. In a separate set of experiments, female SD rats were injected with isoproterenol (ISO) for 5 consecutive days to induce a stress-related status, then CPU86017-RS (80 mg/kg, ig) was administered, and the tissue distributions were examined. The levels of Mn-SOD (manganese containing superoxide dismutase), endoplasmic reticulum (ER) stress sensor proteins (ATF-6, activating transcription factor 6 and PERK, PRK-like ER kinase) and activation of NADPH oxidase (NOX) were detected with Western blotting. Rat liver microsomes were incubated under N<sub>2</sub> for *in vitro* study.

**Results:** The C<sub>max</sub>, t<sub>1/2</sub>, MRT (mean residence time) and AUC (area under the curve) of CPU86017-RS were significantly increased in the hypoxic rats receiving the 3 different doses of CPU86017-RS. The hypoxia-induced alteration of PK was associated with significantly reduced Mn-SOD level, and increased ATF-6, PERK and NOX levels. In ISO-treated rats, the distributions of CPU86017-RS in plasma, heart, kidney, and liver were markedly increased, and NOX levels in heart, kidney, and liver were significantly upregulated. Co-administration of the NOX blocker apocynin eliminated the abnormalities in the PK and tissue distributions of CPU86017-RS induced by hypoxia/oxidative stress. The metabolism of CPU86017-RS in the N<sub>2</sub>-treated liver microsomes was significantly reduced, addition of N-acetylcysteine (NAC), but not vitamin C, effectively reversed this change.

**Conclusion:** The altered PK and metabolism of CPU86017-RS induced by hypoxia/oxidative stress are produced by mitochondrial abnormalities, NOX activation and ER stress; these abnormalities are significantly alleviated by apocynin or NAC.

**Keywords:** CPU86017-RS; antiarrhythmic agents; pharmacokinetics; hypoxia; isoproterenol; ER stress; NADPH oxidase; mitochondria; apocynin; N-acetylcysteine

Acta Pharmacologica Sinica (2013) 34: 1575–1584; doi: 10.1038/aps.2013.94; published online 14 Oct 2013

## Introduction

The pharmacokinetics (PK), distribution and metabolism of drugs can be altered by subcellular changes that result from exposure to intermittent hypoxia, due to oxidative stress. Cell damage induced by hypoxia/oxidative stress results from a series of reactions including the generation of dysfunctional mitochondria (MITO) in which reactive oxygen species (ROS) are produced<sup>[1]</sup>. Therefore, the subcellular damage by hypoxia/oxidative stress manifests itself in the formation of dysfunctional MITO and an excess of ROS that might alter the PK and metabolism of drugs.

MITOs are important subcellular organelles that are susceptible to hypoxic injury. The electron transfer chain (ETC) in MITO has been increasingly recognized as the initial source of ROS<sup>[2,3]</sup>, which promotes the redox-based activation of genesis of reactive oxygen and nitrogen species (RONS) by enzyme-specific “redox switches”<sup>[4]</sup>. ROS formed by dysfunctional MITO, in turn, activate NADPH oxidase (NOX). The activation of NOX is a critical step that amplifies the burden of oxidative stress and impairs the function of the endoplasmic reticulum (ER) through the appearance of ER stress. Mn-SOD, also known as SOD<sub>2</sub> (superoxide dismutase 2), is specifically distributed in MITO and acts as an important factor that reflects the redox system in MITO. It indicates that the MITOs are dysfunctional when the activity of Mn-SOD is decreased. Mn-SOD is related to the entire function of the MITO; it regulates not only the redox system, but also the pleiotropic activ-

<sup>#</sup> These authors contributed equally to this work.

<sup>\*</sup> To whom correspondence should be addressed.

E-mail dezaidai@vip.sina.com

Received 2013-01-24 Accepted 2013-06-24

ity of MITO in maintaining normal cell function and cell survival<sup>[5, 6]</sup>.

In the elderly population, alterations in the PK and distribution of therapeutic agents are increasingly becoming points of concern<sup>[7, 8]</sup>. A decline in mitochondrial function, the presence of oxidative stress and an increase in ER stress chaperones have been found in aged persons<sup>[2, 9]</sup>. Aging cells show abnormalities in the aforementioned biomarkers: dysfunctional MITO, NOX and ER stress, which are found in cells exposed to hypoxia<sup>[10, 11]</sup> or oxidative stress caused by Isoproterenol (ISO)<sup>[12, 13]</sup>. In general, activation of NOX and upregulation of ER stress chaperones are likely the downstream results of MITO dysfunction. These three molecular changes may be tightly linked to form a common pathway in which suppression of one may relieve the other two leading to an improvement in abnormal cellular reactions.

These redox switches might affect the activity of drug-related enzymes in the liver. Furthermore, the redox system in the liver also is changed by aging<sup>[14]</sup>. Drugs are metabolized in the liver by the cytochrome P450 enzymes, which eliminate xenobiotics by detoxification. The liver is susceptible to hypoxia and mitochondrial dysfunction develop, and the activity of P450 is reduced resulting in decreased drug metabolism<sup>[15]</sup>. Mitochondrial dysfunction may be manifested by an altered redox system, a decrease in ATP synthesis and various molecular abnormalities in cells<sup>[16]</sup>.

CPU86017 is a compound derived from berberine that possesses pharmacological activity against cardiac arrhythmia and pulmonary arterial hypertension<sup>[17]</sup>. There are two chiral centers (7N, 13α) in this moiety (Figure 1), so CPU86017 can be derived by chiral separation into 4 isomers: SS, SR, RS and RR, respectively<sup>[18, 19]</sup>. We hypothesized that the PK, rate of metabolism and distribution of CPU86017-RS (RS) could be altered on exposure to intermittent hypoxia and oxidative stress in response to ISO through mitochondrial dysfunction and ER stress. In addition, we suggest that these changes are likely the consequence of activated NOX<sup>[12, 20]</sup>. Thus, we further hypothesized that an administration of either a NOX inhibitor, apocynin, or a potent antioxidant, NAC (N-acetylcysteine), could relieve the abnormalities in the PK and metabolism of RS caused by either hypoxia or ISO injection.

## Materials and methods

### Drugs and reagents

CPU86017-RS (the RS isomer of CPU86017, RS) (Figure 1) and tetra-hydro-berberine (THB, internal standard) were synthesized and provided by the Department of Medicinal Chemistry, China Pharmaceutical University. N-acetylcysteine (NAC) and apocynin (APO, an inhibitor of NADPH oxidase) were purchased from Sigma-Aldrich, Inc (St Louis, USA). Vitamin C was supplied by Wuhan Tongxing Biotechnology Co, Ltd. ISO injection was obtained from Tian-Feng Pharmaceutical Co, Ltd (Shanghai, China). Chromatographically pure methanol was supplied by Jiangsu Hanbang Technology Co, Ltd (Lot 102932, 110556). Dichloromethane was obtained from Nanjing Chemical Instrument Co, Ltd (Lot 10071510738, 10111711246).

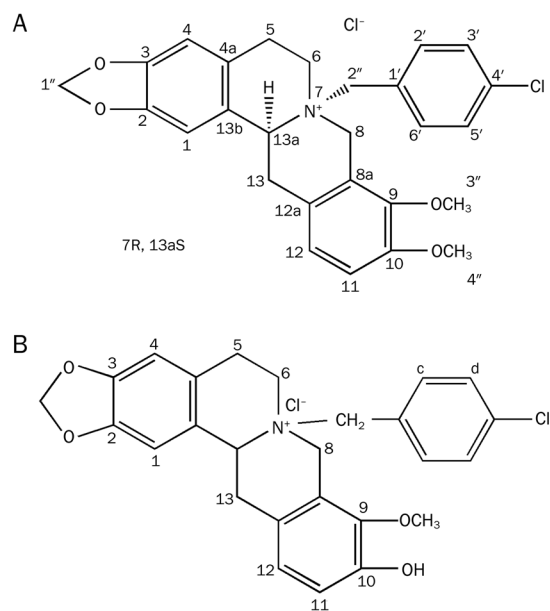


**Figure 1.** Chemical structure of (7R, 13aS)-CPU86017 (RS) (A) and its metabolite (RS - C<sub>10</sub>-OH) (B).

The Coomassie brilliant blue protein assay kit was purchased from Nanjing Jiancheng Bioengineering Institute.

### Instruments

The oxygen analyzer, type CY-12C was from Meicheng Electrochemical Analytical Instrument Factory (Jiande, China). The high performance liquid chromatograph LC-10AT and the ultraviolet detector SPD-10A were purchased from SHIMADZU, Japan. The Type N2000 chromatographic workstation was obtained from Zhejiang University Intelligent Information Engineering Research Institute. The chromatographic column Phecda C18 (150 mm×4.6 mm, 5 μm) was from Jiangsu Hanbang Technology Co, Ltd.

### Experimental animals

Sprague-Dawley rats, weighing 200–220 g, were purchased from the Experimental Animal Center of Zhejiang Province, Hangzhou (license No: SCXK(Zhe) 20080033). Procedures using experimental animals were conducted in accordance with the Experimental Animal Handling Act established by the Science-Technology Bureau of Jiangsu Province, China.

### HPLC assay of RS in plasma

#### Chromatographic conditions<sup>[21, 22]</sup>

LC-10AT HPLC set (SHIMADZU, Japan); SPD-10A ultraviolet detector (SHIMADZU, Japan) and chromatographic column Phecda C18 (150 mm×4.6 mm, 5 μm, Jiangsu Hanbang Technology Co, Ltd) with mobile phase: methanol: pH 4.5 acetate buffer solution (v/v)=57:43; detection wavelength: 234 nm and flow rate: 1 mL/min. The column temperature was set at 35°C.

### Blood samples

Blood samples were collected, and RS was extracted as previously described<sup>[22]</sup>. An aliquot (100  $\mu$ L) of plasma was available after centrifugation of the coagulated blood sample. It was transferred to a test tube containing 40  $\mu$ L of THB (2  $\mu$ g/mL) and mixed. In biological samples, 5 mL of dichloromethane was added to extract RS and the sample was vortexed for 5 min. The sample was then centrifuged (3500 r/min, 15 min) again, and 4 mL of the lower organic layer was transferred into another tube. The organic solvent was evaporated by placing tubes into a hot water bath at 55°C. The dried sample was dissolved into a 50- $\mu$ L mobile phase, and an aliquot of 20  $\mu$ L was retained for injection into the HPLC system.

### Calibration curve

Stock solutions of RS (100  $\mu$ g/mL) and THB (40  $\mu$ g/mL) were prepared in methanol and stored at 4°C, and the calibration curve of RS was produced as described<sup>[22]</sup> by dissolving the stock solution in blank rat plasma, pooled tissue blank, and liver microsomes, yielding final concentrations of 10, 33, 100, 333, 1000, 3333, and 10000 ng/mL. The internal standard of RS was plotted by setting the peak area ratio as the ordinate (Y) with the RS concentration on the abscissa (X). Calibration curves were produced for measuring RS in plasma, liver microsome preparations and pooled tissue extracts.

### Method validation

The selectivity of the method was determined using blank plasma samples from 3 different quality control (QC) samples (100, 333, and 1000 ng/mL); the samples were pretreated and analyzed. The recovery of RS was assessed using the QC samples mixed with THB; the ratio of the measured concentration and the theoretical concentration of RS were calculated. The intra- and inter-day precision (expressed as relative standard deviation, RSD) were assessed by assaying 3 replicate QC samples on five different days. The lowest detectable limit (LDL) was assessed by assaying 5 different samples. The response of RS was at least 3 times more than the baseline noise.

### PK parameters

Thirty-eight male Sprague-Dawley rats, 6 weeks old, were randomly divided into 7 groups. Normal rats (N) and rats exposed to intermittent hypoxia (10% O<sub>2</sub>) 8 h/d for 7 d were treated with 3 doses of RS as the following: normal rats treated ig with low dose (N+RSL, 20 mg/kg), medium dose (N+RSM, 40 mg/kg) and high dose (N+RSH, 80 mg/kg) RS; and hypoxic rats (H) treated ig with low dose (H+RSL, 20 mg/kg), medium dose (H+RSM, 40 mg/kg) and high dose (H+RSH, 80 mg/kg) RS. A dose of the RS compound (RSL, RSM and RSH) was delivered on each of days 4-7. On the day 8, the same dose of RS (80 mg/kg, ig) was administered and blood samples were collected from the post-orbital venous plexus at 10 min, 20 min, 1, 1.5, 2, 4, 6, 8, 12, and 24 h. The 7th group of rats was treated with apocynin (80 mg/kg, ig) on day 1-7. Blood samples were collected and centrifuged (10000 r/min,

10 min, 4°C), and the plasma was transferred to clean centrifuge tubes for the HPLC assay<sup>[21]</sup>.

The data were entered into the BAPP 2.0 software to calculate the drug concentrations. The pharmacokinetic parameters were calculated using a non-compartmental model. The peak concentration of drug ( $C_{max}$ ) and the peak time of drug ( $T_{max}$ ) were determined from the observations. The elimination rate constant (K) was calculated from linear regression of the terminal portion of the blood drug concentration-time curve. The elimination half-life ( $t_{1/2}$ ) was calculated using the equation,  $t_{1/2}=0.693/K$ . The blood drug concentration-time area under the curve was calculated by the trapezoidal method. Mean residence time (MRT) was calculated from  $MRT=AUMC/AUC$ , (AUMC-area under moment curve).

### Metabolism of RS by a liver microsome preparation *in vitro*

Procedures for measuring the rate of metabolism of RS are based on a previous study<sup>[23]</sup> with minor changes. Six male Sprague-Dawley rats were sacrificed, and livers were harvested and washed with cold physiological saline. CPU86017 is metabolized in the liver by a demethylation reaction at the C10 position (from -OCH<sub>3</sub> to -OH)<sup>[24]</sup>. Twenty grams of liver tissue was accurately weighed and added to 10 volumes of K-H solution pre-cooled to 4°C ( $v/v=1/5$ ); this step was followed by homogenization in an ice-water bath. The homogenate was centrifuged at 9000 $\times$ g at 4°C for 15 min, and the supernatant containing microsomes was transferred to clean centrifuge tubes. The liver microsomal protein content was determined by the Coomassie brilliant blue method according to the manufacturer's instructions. An aliquot (20 mL) of the liver microsome homogenate was incubated in a thermostatic water bath at 37°C. The normal group samples were maintained in an atmosphere of pure oxygen, and N<sub>2</sub> was driven into the medium to produce a status of hypoxia for the hypoxia group samples. Liver microsome preparations were incubated for 60 min with RS ( $3\times 10^{-7}$  mol/L) in the presence or absence of drug treatment (vitamin C or NAC). The concentration of RS was assayed to monitor the amount of RS remained in samples from the following 6 groups ( $n=6$ ): normal (N), hypoxia (Hyp), hypoxia and treatment with anti-oxidants: Hyp+VcL (vitamin C,  $10^{-6}$  mol/L), Hyp+VcH (vitamin C,  $10^{-5}$  mol/L), Hyp+NACL (N-acetylcysteine,  $10^{-6}$  mol/L), and Hyp+NACH (N-acetylcysteine,  $10^{-5}$  mol/L). An aliquot of 0.5 mL liver microsome sample was taken for assay at the following times: 0, 20, 40, and 60 min after drug treatment. Finally, the remaining of RS in the sample was determined using the HPLC conditions described earlier.

### Changes in RS disposition under stress

Female Sprague-Dawley rats weighing 200-220 g were placed under a stress-related status induced by ISO 1 mg/kg, *sc*, for 5 d<sup>[12, 13]</sup>, and treated orally with 80 mg/kg APO for each of the last 3 d. The concentrations in the plasma, heart, kidney, and liver were determined 4 h after single administration of RS (80 mg/kg, ig).

### Western blotting of NOX in tissues

The protein expression of the catalytic and modulating subunits of NOX, such as p67<sup>phox</sup>, Nox2 (gp91<sup>phox</sup>), and Nox4 in the heart, kidney and liver, was measured by Western blotting as previously reported<sup>[13]</sup>. Briefly, 50 mg fresh tissue was added to 0.5 mL RIPA lysis buffer and homogenized on ice. The homogenate liquid was centrifuged at 10 000×g for 20 min at 4°C. The protein concentrations of supernatants from the heart, kidney and liver were determined using a Coomassie brilliant blue protein kit (Jiancheng Technology Company, Nanjing, China). After SDS-PAGE electrophoresis, the proteins were transferred to a nitrocellulose membrane and incubated with primary antibodies (1:200–1000 dilution, 37°C, 1–2 h). The primary antibodies against Nox2, Nox4, and p67<sup>phox</sup> were from Santa Cruz, USA. The β-actin antibody was from Wuhan Boster Biological Engineering Co, Ltd, China. After being washed with TBST three times, the membranes were incubated with horseradish peroxidase-conjugated secondary antibody (1:200, 37°C, 1–2 h, Wuhan Boster Biological Technology, China) and were washed with TBST. Antigen was detected with a 3,3'-DiAMGnobenzidine (DAB) kit. A linear relationship between blot density and protein load was observed when 20, 40, 60, 80, and 100 μg of membrane protein were used per lane. Data were compared among the normal, ISO-treated and APO-treated rats.

### Statistical analysis

Data are presented and compared as the mean±SD. The software package SPSS 11.5 (USA) was used for the analysis. One-way analysis of variance was used, followed by Dunnett's test. The Student Newman Keuls test was performed when the variances were equal, and the Games-Howell test was performed when the variances were not equal. The results were considered statistically significant when the probability was  $P < 0.05$ .

## Results

### HPLC assay

The specificity of the assay methodology was evaluated by analyzing the individual blank plasma sample from the six different sources. All of the samples were found to have no interference from endogenous substances on the retention times of RS or THB, which were 9.7 min and 12.7 min, respectively. Typical chromatograms of the blank plasma and a plasma/tissue sample spiked with RS and THB from different groups are shown in Figure 2.

Standard curves and the precision of the HPLC assay: An internal standard of RS was plotted by the peak area ratio. The serum standard curve was obtained after linear regression ranging from 10 ng/mL to 10 000 ng/mL. The distribution of RS in tissues was measured in pooled tissue samples using a calibration curve. A range of 10 ng/mL to 1000 ng/mL RS was applied to liver microsome preparations.

Equations of linear regression for measuring RS in plasma, liver microsome preparations, and the distribution in tissues

(by use of the pooled tissue blank) were  $y = 0.0005x + 0.088$  ( $r = 0.999$ ),  $y = 0.0061x - 0.0299$  ( $r = 0.999$ ) and  $y = 0.0006x + 0.0697$  ( $r = 0.9936$ ), respectively.

The recovery rate was 94.1% to 103.7%, and the intra-day and inter-day precision was 5.9% and 6.6%, respectively. The limitation of detection was 7.56 ng/mL for the HPLC assay.

### Altered PK values induced by hypoxia

Plasma concentration-time curves of RS in the 6 groups were plotted and compared between the normoxic and hypoxic groups for the low, middle and high doses separately. The plasma levels of RS were significantly higher ( $P < 0.01$ ) in the hypoxic group than those in the normal group. The curves for the low, middle and high doses were in parallel for the hypoxic and normoxic rats (Figure 3A–3C).

The data of the plasma concentration-time curves in the 6 groups were entered into the BAPP2.1 program and fitted with a two-compartment model of extravascular administration. The PK parameters were calculated and compared between hypoxia and normoxia (Tables 1–3). In hypoxic rats, the  $C_{max}$ ,  $T_{max}$ ,  $t_{1/2}$ , MRT, and AUC values were significantly increased ( $P < 0.05$  or  $P < 0.01$ ) and the K values were reduced compared with the normoxic rats. Thus, it is clear that hypoxia alters the pharmacokinetic behavior of RS in rats (Figure 3).

### APO alleviates the hypoxia-altered PK

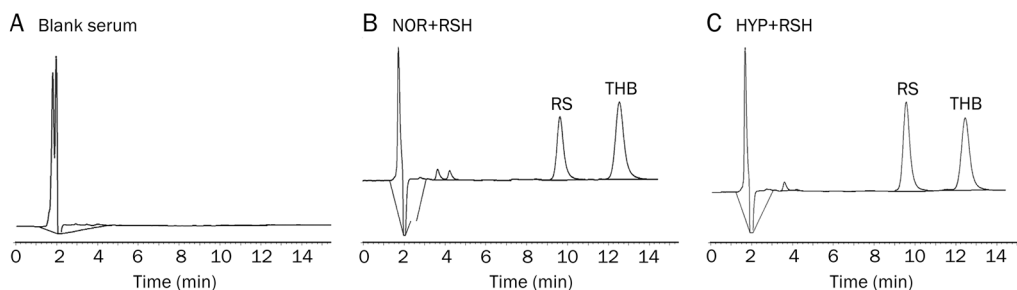
Upon exposure to intermittent hypoxia, the PK of RS was significantly altered, showing elevated plasma levels and an increase in MRT in rats. In an additional group, APO was used to test whether suppression of NOX could reverse these changes. Following APO administration, the plasma-time profile of RS was monitored and the changes in plasma levels were alleviated significantly ( $P < 0.01$ ), compared to the hypoxia-untreated animals (Figure 3D); in addition, the PK parameters were significantly relieved (Table 4).

**Table 1.** Pharmacokinetic parameters of CPU86017-RS (RSL, 20 mg/kg) are compared between the normal and hypoxia. Mean±SD.  $n = 6-7$ . <sup>b</sup> $P < 0.05$ , <sup>c</sup> $P < 0.01$  vs Normal.

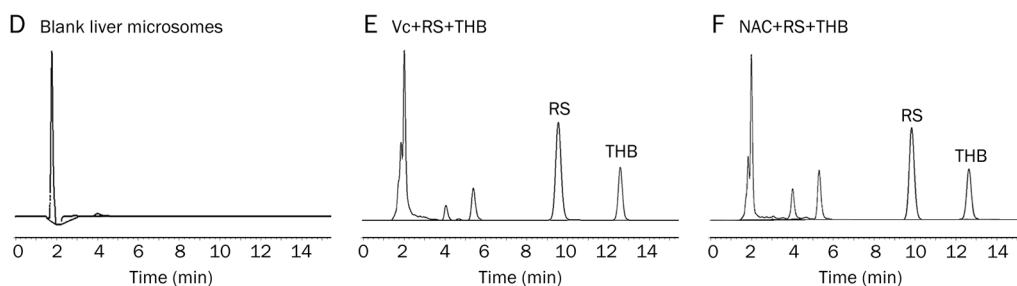
Pharmacokinetic parameters	Normal+RSL	Hypoxia+RSL
$C_{max}$ (ng/mL)	153±18	223±36 <sup>c</sup>
$T_{max}$ (min)	60	90
K ( $\text{min}^{-1}$ )	0.0013±0.0002	0.0010±0.0001 <sup>b</sup>
$t_{1/2}$ (min)	565±86	676±66 <sup>b</sup>
MRT (min)	803±114	960±58 <sup>b</sup>
AUC <sub>0-t</sub> ( $\mu\text{g}\cdot\text{min}\cdot\text{L}^{-1}$ )	67 202±6252	91 842±9706 <sup>c</sup>
AUC <sub>0-∞</sub> ( $\mu\text{g}\cdot\text{min}\cdot\text{L}^{-1}$ )	81 647±7315	105 035±10 176 <sup>c</sup>
AUMC ( $\mu\text{g}\cdot\text{min}^2\cdot\text{L}^{-1}$ )	66 237 668±15 907 095	100 687 218±1 067 811 <sup>c</sup>

$C_{max}$ , maximum concentration;  $T_{max}$ , time to maximum concentration; K, the elimination rate constant;  $t_{1/2}$ , half-life; MRT, the mean residence time; AUC, the area under concentration-time curve; AUMC, the area under the first moment of the plasma concentration-time curve.

## Experiment 1: Determining the PK of RS



## Experiment 2: Determining RS metabolism in liver microsome preparation



## Experiment 3: Determining RS distribution

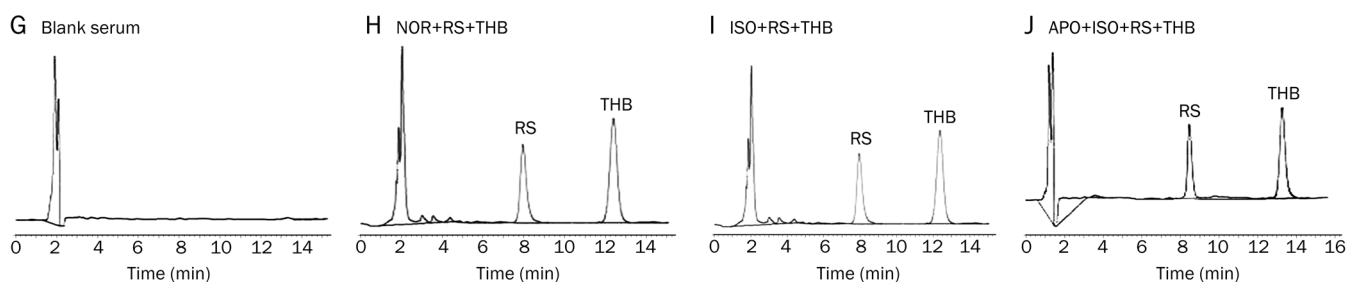


**Figure 2.** HPLC chromatograms of RS in rat serum, liver microsome and tissue pooled samples in 3 separate experiments. Experiment 1, plasma levels-time curves and PK parameters: (A) Blank rat serum; (B) Serum sample from normal rat administered by RS 80 mg/kg ig, mixed with the internal standard tetra-hydrogen-berberine (THB); (C) Serum from hypoxic rat administered with RS. Experiment 2, RS metabolism in liver microsome preparation: (D) Blank rat liver microsome; (E) Vitamin C (Vc) treated; (F) N-acetyl-cysteine (NAC) treated. Experiment 3, tissue distribution of RS: (G) Pooled tissue blank; (H) Pooled tissue sample from normal rat administered with RS; (I) Pooled sample from ISO treated rats; (J) Pooled sample from APO (apocynin)+ISO treated rats.

**Table 2.** Pharmacokinetic parameters of CPU86017-RS (RSM, 40 mg/kg) are compared between the normal and hypoxia. Mean±SD.  $n=6-7$ . <sup>b</sup> $P<0.05$ , <sup>c</sup> $P<0.01$  vs Normal.

Pharmacokinetic parameters	Normal+RSM	Hypoxia+RSM
$C_{max}$ (ng/mL)	298±38	476±86 <sup>c</sup>
$T_{max}$ (min)	60	90
$K$ ( $\text{min}^{-1}$ )	0.0013±0.0002	0.0010±0.0001 <sup>b</sup>
$t_{1/2}$ (min)	565±86	694±107 <sup>b</sup>
MRT (min)	677±105	995±106 <sup>b</sup>
$AUC_{0-t}$ ( $\mu\text{g}\cdot\text{min}\cdot\text{L}^{-1}$ )	91415±10652	213824±23358 <sup>c</sup>
$AUC_{0-\infty}$ ( $\mu\text{g}\cdot\text{min}\cdot\text{L}^{-1}$ )	106178±12205	229944±25619 <sup>c</sup>
AUMC ( $\mu\text{g}\cdot\text{min}^2\cdot\text{L}^{-1}$ )	72175700±15719426	94976459±9499675 <sup>b</sup>

**Table 3.** The pharmacokinetic parameters of CPU86017-RS (RSH, 80 mg/kg) are compared between the normal and hypoxia. Mean±SD.  $n=6-7$ . <sup>b</sup> $P<0.05$ , <sup>c</sup> $P<0.01$  vs Normal.

Pharmacokinetic parameters	Normal+RSH	Hypoxia+RSH
$C_{max}$ (ng/mL)	596±125	934±63 <sup>c</sup>
$T_{max}$ (min)	60	90
$K$ ( $\text{min}^{-1}$ )	0.0014±0.0003	0.0011±0.0001 <sup>b</sup>
$t_{1/2}$ (min)	509±111	649±79 <sup>b</sup>
MRT (min)	766±100	950±87 <sup>c</sup>
$AUC_{0-t}$ ( $\mu\text{g}\cdot\text{min}\cdot\text{L}^{-1}$ )	229975±41042	352471±29276 <sup>c</sup>
$AUC_{0-\infty}$ ( $\mu\text{g}\cdot\text{min}\cdot\text{L}^{-1}$ )	249222±39697	389918±40857 <sup>c</sup>
AUMC ( $\mu\text{g}\cdot\text{min}^2\cdot\text{L}^{-1}$ )	100028056±20214538	145470390±22115370 <sup>c</sup>

### Hypoxia induces dysfunctional MITO, ER stress, and NOX

The PK parameters of RS were significantly altered by hypoxia. Therefore, it was important to determine whether these changes were related to oxidative stress status, mitochondrial dysfunction or an increase in ER stress chaperones in organs related to drug transformation and elimination. In the hypoxic liver, the elevation in hepatic MDA and the decrease in Mn-SOD were significant ( $P < 0.01$ ). There was also a significant increase in ER stress sensor proteins, specifically ATF-6 and PERK, compared to normal rats ( $P < 0.01$ ). Furthermore, there was an increase in the MDA and a decrease in Mn-SOD, which were accompanied by an elevation in NOX and  $p22^{\text{phox}}$  in the hypoxic kidney, compared to the normal rats ( $P < 0.01$ ). Interestingly, these effects were mitigated significantly by APO (Figure 4).

**Table 4.** Pharmacokinetic parameters of RSM are compared between APO treated and untreated groups exposed to hypoxia. Means  $\pm$  SD.  $n = 6$ .  $^{\circ}P < 0.01$  vs Hypoxia.

Pharmacokinetic parameters	Hypoxia+RSM	APO+Hyp+RSM
$C_{\text{max}}$ (ng/mL)	476 $\pm$ 88	337 $\pm$ 47 $^{\circ}$
$T_{\text{max}}$ (min)	90	90
$K$ ( $\text{min}^{-1}$ )	0.0010 $\pm$ 0.0001	0.0013 $\pm$ 0.0001 $^{\circ}$
$t_{1/2}$ (min)	694 $\pm$ 107	521 $\pm$ 53 $^{\circ}$
MRT (min)	995 $\pm$ 106	542 $\pm$ 54 $^{\circ}$
$\text{AUC}_{0-t}$ ( $\mu\text{g}\cdot\text{min}\cdot\text{L}^{-1}$ )	213 824 $\pm$ 23 358	139 036 $\pm$ 4767 $^{\circ}$
$\text{AUC}_{0-\infty}$ ( $\mu\text{g}\cdot\text{min}\cdot\text{L}^{-1}$ )	229 944 $\pm$ 25 619	150 947 $\pm$ 6921 $^{\circ}$
AUMC ( $\mu\text{g}\cdot\text{min}^2\cdot\text{L}^{-1}$ )	94 976 459 $\pm$ 9 499 675	75 401 163 $\pm$ 8 148 517 $^{\circ}$

### Metabolizing rate of RS under hypoxia *in vitro*

The metabolism of RS in the hepatic microsome preparations was measured *in vitro* by determining the remaining amount of RS in the medium. Under normal conditions, the RS content declined owing to the formation of the demethylated compound, as shown in Figure 1. The remaining of RS in the liver microsome preparation was increased significantly when the medium was exposed to hypoxia ( $P < 0.01$ ), indicating that a slowing of the metabolic reaction had taken place in the hypoxic microsome medium. When the two antioxidants were added into the medium, a significant decrease in the remaining of RS occurred in the group receiving NAC ( $P < 0.01$ ) compared with the untreated hypoxic group. In contrast, the effectiveness of ascorbic acid was mild and did not reach statistical significance (Figure 5).

### Changes in RS distribution by ISO

An increase in plasma levels of RS was found in rats exposed to intermittent hypoxia. This phenomenon is likely due to oxidative stress induced by intermittent hypoxia. Therefore, we tested whether an episode of oxidative stress induced by APO could affect the plasma concentration and distribution of RS in

tissues. A stress-related condition was induced by ISO treatment (1 mg/kg, *sc*) for 5 d<sup>[13]</sup>, and during the last 3 days, apocynin, an inhibitor of NOX, was administered (80 mg/kg, *ig*). The levels of RS in the plasma, heart, kidney and liver were elevated significantly relative to the normal condition ( $P < 0.01$ ), which were likely secondary to the oxidative status in the ISO-injected rats. These changes disappeared in the groups treated with APO, compared with the untreated groups ( $P < 0.01$ ) (Figure 6).

### NOX protein upregulated by ISO

An assay of NOX protein in the heart, kidney and liver was conducted to examine the possibility that the catalytic ( $p67^{\text{phox}}$ ) and modulating subunits (Nox2, Nox4) of NOX were overexpressed in ISO-treated rats. Interestingly, these abnormalities were significantly ameliorated by an application of APO, which blocks NOX activity ( $P < 0.01$ ), compared with the untreated rats (Figure 7).

### Discussion

Following hypoxia exposure, an increase in the plasma-time profile for RS was found in association with an increase in the  $C_{\text{max}}$ ,  $T_{\text{max}}$ ,  $t_{1/2}$ , MRT, and AUC, but there was a reduction in the  $K$  values relative to normoxic controls. Pharmacokinetic parameters among the 3 doses were in parallel, indicating that the metabolism of RS in rats follows first-order kinetics. The elevations in plasma levels were significant, implying that the elimination of RS is impaired by hypoxia. In a separate experiment, an increase in the plasma levels of RS was produced in ISO-injected rats and the concentrations in the heart, kidney and liver were significantly increased; these effects were alleviated by APO through a blockade of NOX. These findings are in line with the effectiveness of application of APO in attenuating hypoxic pulmonary hypertension<sup>[25]</sup>, the impaired function of organs in response to hypoxia<sup>[10, 11]</sup>, and the cardiac failure observed in ISO-injected rats<sup>[12, 13]</sup>.

Pharmacokinetics, metabolism and drug distribution can be altered by inflammatory reactions through modulation of the hepatic flavin monooxygenases, UDP-glucuronosyl transferases, sulfotransferases, and glutathione S-transferases, as well as hepatic transporters<sup>[15]</sup>. These changes are frequently accompanied by an excess of ROS, pro-inflammatory factors and activated NOX<sup>[3, 26, 27]</sup>, all of which are consequences of mitochondrial dysfunction. Drug metabolism is an energy-consuming process that is linked to mitochondria by the need for ATP. This process is impaired under conditions that result in a lack of oxygen supply, such as sepsis<sup>[28]</sup>. Oxygen-dependent metabolism of RS was confirmed in liver microsome preparations gassed with  $\text{N}_2$  *in vitro*. The enzymatic elimination of RS in the liver requires an oxygen supply that is reduced by hypoxia and the oxidative stress caused by ISO administration. Therefore, a reduction in the hepatic elimination of RS caused elevated levels of RS in the plasma and tissue. The enzymatic transformation of RS involves a demethylating reaction of the berberine molecule at the  $\text{C}_{10}$  position by converting  $-\text{OCH}_3$  to  $-\text{OH}$  (Figure 1)<sup>[24]</sup>, and this is the

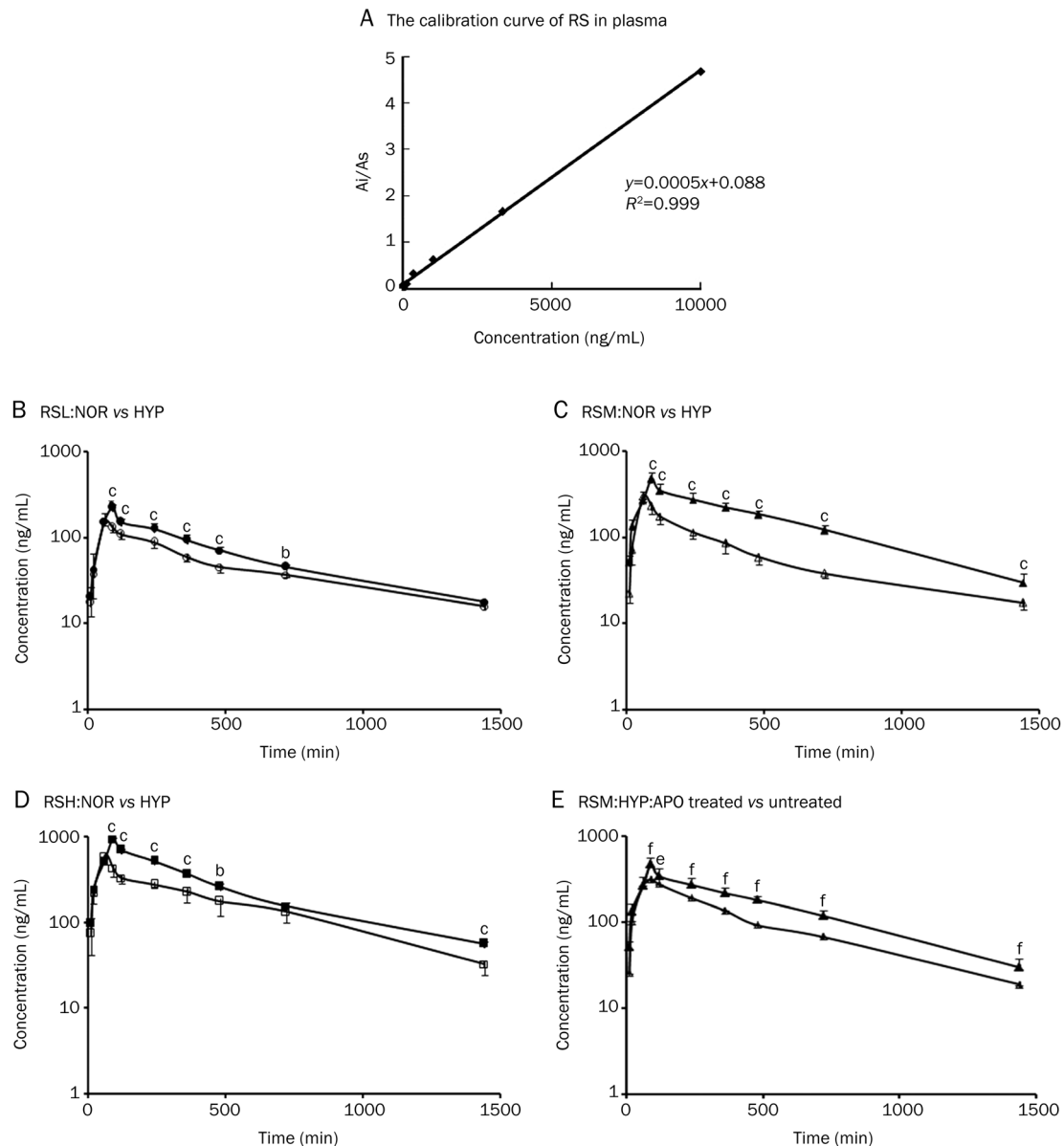


**Figure 3.** Concentration-time curves of 3 doses RS in plasma were compared between normal (NOR) and hypoxic (HYP) rats. (A) The calibration curve. Ai: peak area of RS; As: peak area of THB; Comparison between the hypoxic against normal; (B) RSL (20 mg/kg, ig): ○, NOR+RSL; ●, HYP+RSL; (C) RSM (40 mg/kg, ig): △, NOR+RSM; ▲, HYP+RSM; (D) RSH (80 mg/kg, ig): □, NOR+RSH; ■, HYP+RSH; (E) Comparison between the APO treated against the untreated hypoxic rats. HYP+RSM (40 mg/kg, ig): ▲, HYP+RSM (upper); ▲, APO+HYP+RSM (below).  $n=6-7$ . Mean±SD. <sup>a</sup> $P<0.05$ , <sup>c</sup> $P<0.01$  vs NOR. <sup>e</sup> $P<0.05$ , <sup>f</sup> $P<0.01$  vs APO+HYP+RSM.

Phase 1 of the drug's metabolism oxygen dependent. Hypoxia interferes with the Phase 1 metabolism of many therapeutic agents in the liver<sup>[29]</sup>. At the same time, an excess of oxidants impairs protein biosynthesis by the unfolded protein response, which increases the levels of the ER stress chaperones, namely ATF-6 and PERK, and the function of cells is also seriously impaired<sup>[30]</sup>. It also alters the bioactive molecules responsible for the metabolism of drugs by downregulating hepatic CYP1A1, 1A2, 2B4, 2C5, and 2C16 and upregulating CYP3A6 and P-glycoprotein in the liver<sup>[31]</sup>.

Under conditions of hypoxia, ROS are first generated from

the abnormal oxidative phosphorylation system at complex I in mitochondria; then, superoxide ( $O_2^{\cdot-}$ ) can be converted into either  $H_2O_2$  or  $ONOO^{\cdot-}$  by Mn-SOD<sup>[32]</sup>. An increase in ROS indicates oxidative stress, in general, and a reduction in Mn-SOD and mitochondrial impairment, in particular<sup>[33]</sup>. By suppressing NOX, APO greatly relieves mitochondrial impairment and the abnormal PK, and thus achieves normal drug metabolism and distribution. For the activation of NOX, stimulators, such as ET-1, AII,  $TNF\alpha$ , and ROS, are needed. Therefore, suppression on these stimulators leads to an alleviation of the mitochondrial dysfunction and altered PK and drug

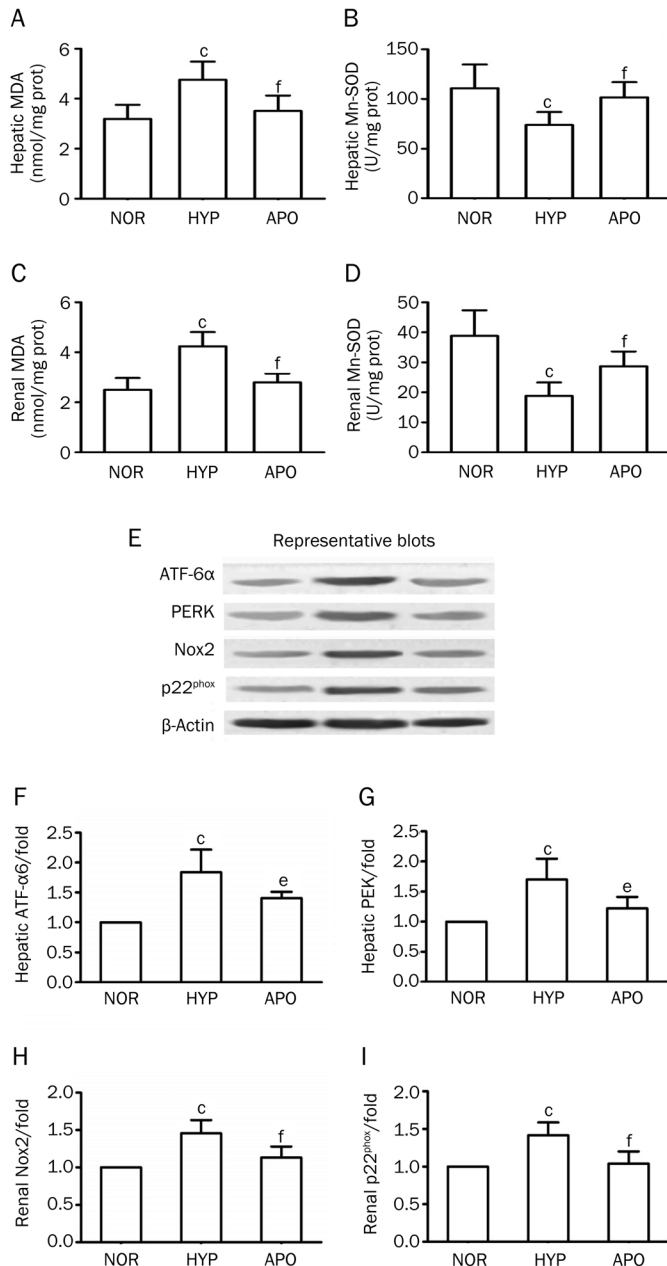


**Figure 4.** Oxidative stress, dysfunctional mitochondria, ER stress and activated NADPH oxidase were dominant in hypoxic liver and kidney and were attenuated by apocynin (APO). (A) Hepatic MDA; (B) Hepatic Mn-SOD; (C) Renal MDA; (D) Renal Mn-SOD; (E) Representative Bands; (F) Hepatic ATF-6 $\alpha$ ; (G) Hepatic PERK; (H) Renal Nox2; (I) Renal p22<sup>phox</sup>.  $n=6$ . Mean $\pm$ SD. <sup>c</sup> $P<0.01$  vs NOR. <sup>e</sup> $P<0.05$ , <sup>f</sup> $P<0.01$  vs HYP.

metabolism in tissues. A decline in drug metabolism (down-regulated CPY1A) was found in hypoxic Atlantic croaker, and these changes were significantly attenuated by Vitamin E<sup>[34]</sup>.

In humans who remained at 4559 m above sea level for 7 d, there was only a small decrease in the activity of CYP2D6 and CYP3A4<sup>[35]</sup>. In contrast, in the present study, rats were kept at 10% $\pm$ 0.5% O<sub>2</sub> for 8 h per day for 7 d, which corresponds to an altitude of more than 6000 m above sea level and causes more

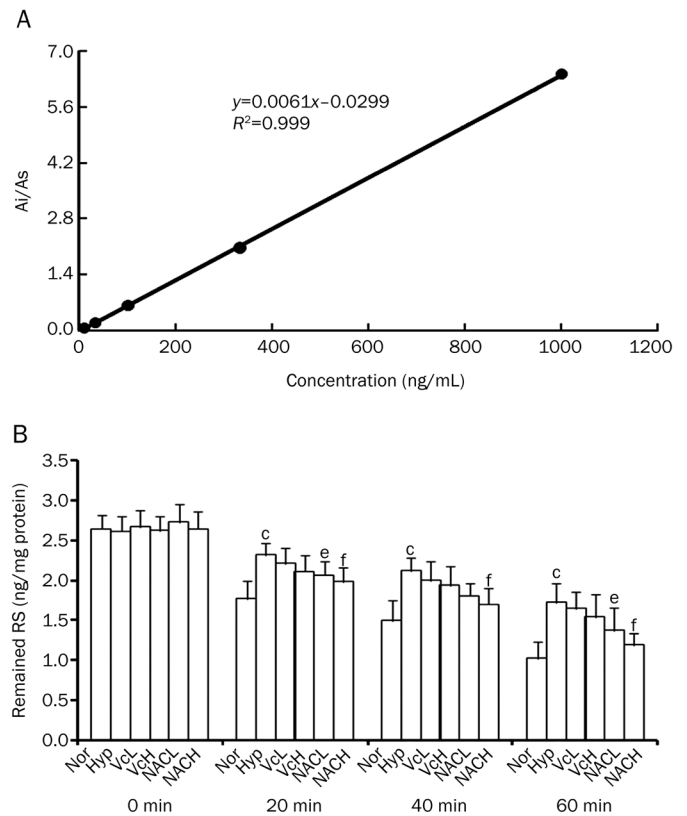


**Figure 5.** The metabolizing rate of RS in rat liver microsome preparation. (A) The calibration curve, Ai: peak area of RS; As: peak area of THB; (B) The metabolism of RS in liver microsome preparation.  $n=6$ . Mean $\pm$ SD. <sup>c</sup> $P<0.01$  vs NOR. <sup>e</sup> $P<0.05$ , <sup>f</sup> $P<0.01$  vs HYP.

significant changes in PK.

Hypoxia induces inflammation linked to an increase in NF $\kappa$ B<sup>[36]</sup>. Both dysfunctional MITO and NOX actively participate in chronic inflammation by producing ROS and pro-inflammatory biomarkers in cells. There is a vicious cycle in ROS production between abnormal MITO and activated NOX in affected cells. Thus, a MITO-NOX pathway may be suggested as a link in affected tissues<sup>[4]</sup> that mediates both ER stress and abnormal cellular responses.

In conclusion, oxidative stress caused by either hypoxia or ISO elicits abnormal PK, metabolism and tissue distribution of RS due to mitochondrial dysfunction, activation of NOX and ER stress. These changes are significantly alleviated by either APO, a blockade of NOX or NAC, a potent antioxidant agent. However, ascorbic acid does not have the same effect. It is interesting to identify a link between abnormal PK and dysfunctional MITO. APO and NAC are potential for a relief of the abnormal PK, drug metabolism and distribution of RS by correcting the dysfunctional MITO and activated NOX in tissues.

#### Acknowledgements

The project is supported by the National Natural Science Foundation of China (No 81070145).

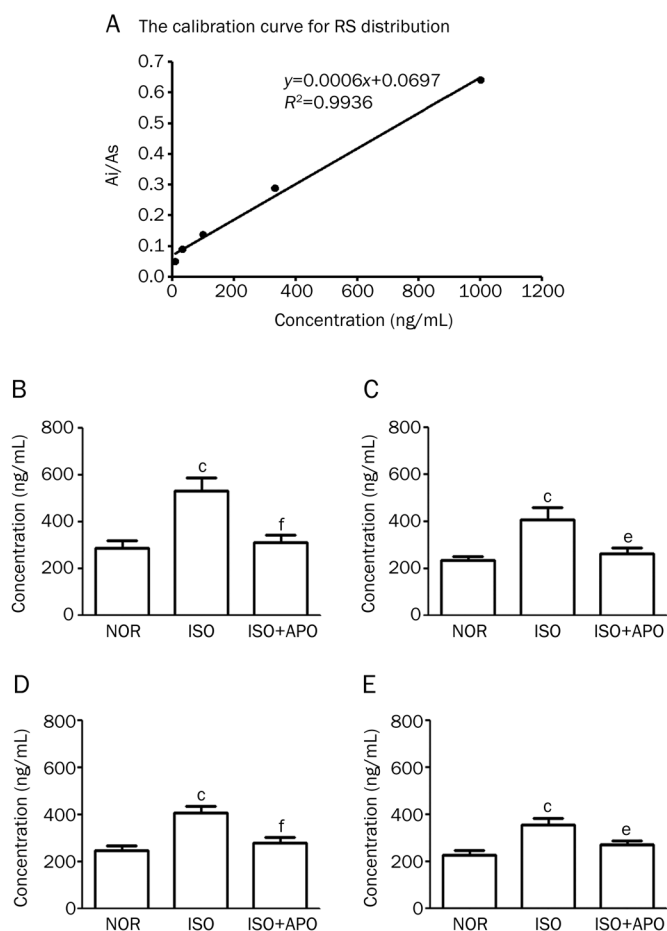


**Figure 6.** An increase in tissue distribution of RS is significant following isoproterenol (1 mg/kg, sc, 5 d) which is alleviated by apocynin (80 mg/kg, in the last 3 d) in rats. (A) The calibration curve in pooled tissue samples, Ai: peak area of RS; As: peak area of THB; (B) Plasma; (C) Heart; (D) Liver; and (E) Kidney. NOR-normal, ISO-isoproterenol, ISO+APO (apocynin).  $n=6$ . Mean $\pm$ SD. <sup>a</sup> $P<0.01$  vs NOR. <sup>b</sup> $P<0.05$ , <sup>f</sup> $P<0.01$  vs ISO.

### Author contribution

Jie GAO conducted the project, processed data and prepared the manuscript; Xuan-sheng DING worked in assistance with the experiment and data processing; Yu-mao ZHANG conducted experiments and managed the data; De-zai DAI and Yin DAI designed the project and prepared and revised the manuscript; Mei LIU participated in the experiment and data

analysis; and Can ZHANG provided the test compounds.

### References

- 1 Ten VS, Starkov A. Hypoxic-ischemic injury in the developing brain: the role of reactive oxygen species originating in mitochondria. *Neurol Res Int* 2012; 2012: 542976.
- 2 Chaudhary KR, El-Sikhry H, Seubert JM. Mitochondria and the aging heart. *J Geriatr Cardiol* 2011; 8: 159–67.
- 3 Kolamunne RT, Clare M, Griffiths HR. Mitochondrial superoxide anion radicals mediate induction of apoptosis in cardiac myoblasts exposed to chronic hypoxia. *Arch Biochem Biophys* 2011; 505: 256–65.
- 4 Schulz E, Wenzel P, Munzel T, Daiber A. Mitochondrial redox signaling: interaction of mitochondrial reactive oxygen species with other sources of oxidative stress. *Antioxid Redox Signal* 2012. doi: 10.1089/ars.2012.4609.
- 5 Folbergrova J, Jesina P, Nuskova H, Houstek J. Antioxidant enzymes in cerebral cortex of immature rats following experimentally-induced seizures: upregulation of mitochondrial MnSOD (SOD2). *Int J Dev Neurosci* 2013; 31: 123–30.
- 6 Candas D, Fan M, Nantajit D, Vaughan AT, Murley JS, Woloschak GE, et al. CyclinB1/Cdk1 phosphorylates mitochondrial antioxidant MnSOD in cell adaptive response to radiation stress. *J Mol Cell Biol* 2013; 5: 166–75.
- 7 Schoen JC, Erlandson KM, Anderson PL. Clinical pharmacokinetics of antiretroviral drugs in older persons. *Expert Opin Drug Metab Toxicol* 2013; 9: 573–88.
- 8 Lafuente-Lafuente C, Baudry E, Paillaud E, Piette F. Clinical pharmacology and aging. *Presse Med* 2013; 42: 171–80.
- 9 Brown MK, Naidoo N. The endoplasmic reticulum stress response in aging and age-related diseases. *Front Physiol* 2012; 3: 263.
- 10 Zhang GL, Dai DZ, Zhang C, Dai Y. Apocynin and raisanberine alleviate intermittent hypoxia induced abnormal StAR and 3beta-HSD and low testosterone by suppressing endoplasmic reticulum stress and activated p66Shc in rat testes. *Reprod Toxicol* 2013; 36: 60–70.
- 11 Liu GL, Yu F, Dai DZ, Zhang GL, Zhang C, Dai Y. Endoplasmic reticulum stress mediating downregulated StAR and 3-beta-HSD and low plasma testosterone caused by hypoxia is attenuated by CPU86017-RS and nifedipine. *J Biomed Sci* 2012; 19: 4.
- 12 Xu J, Li N, Dai DZ, Yu F, Dai Y. The endothelin receptor antagonist CPU0213 is more effective than aminoguanidine to attenuate isoproterenol-induced vascular abnormality by suppressing overexpression of NADPH oxidase [correction of oxidas], ETA, ETB, and MMP9 in the vasculature. *J Cardiovasc Pharmacol* 2008; 52: 42–8.
- 13 Cheng YS, Tang YQ, Dai DZ, Dai Y. AQP4 knockout mice manifest abnormal expressions of calcium handling proteins possibly due to exacerbating pro-inflammatory factors in the heart. *Biochem Pharmacol* 2012; 83: 97–105.
- 14 Wu JL, Wu QP, Peng YP, Zhang JM. Effects of L-malate on mito-

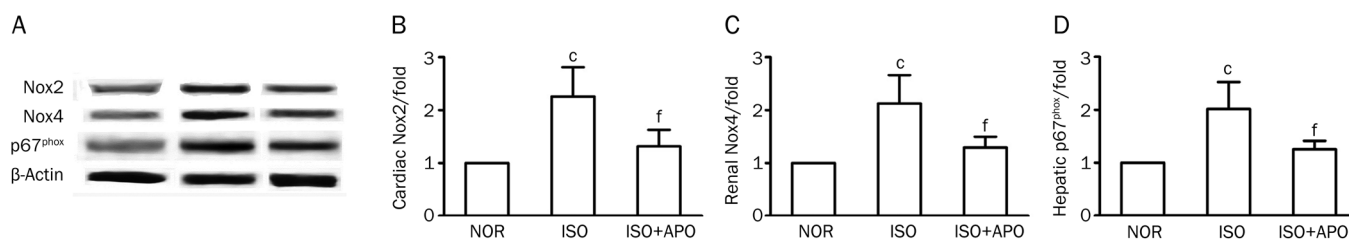


**Figure 7.** Protein distribution of NADPH oxidase in organs is altered by isoproterenol injected in rats. (A) Representative blots; (B) Cardiac Nox2; (C) Renal Nox4; (D) Hepatic p67<sup>phox</sup>.  $n=6$ . Mean $\pm$ SD. <sup>a</sup> $P<0.01$  vs NOR. <sup>f</sup> $P<0.01$  vs ISO.

- chondrial oxidoreductases in liver of aged rats. *Physiol Res* 2011; 60: 329–36.
- 15 Aitken AE, Richardson TA, Morgan ET. Regulation of drug-metabolizing enzymes and transporters in inflammation. *Annu Rev Pharmacol Toxicol* 2006; 46: 123–49.
- 16 Smith RA, Hartley RC, Cocheme HM, Murphy MP. Mitochondrial pharmacology. *Trends Pharmacol Sci* 2012; 33: 341–52.
- 17 Dai DZ. CPU86017: a novel Class III antiarrhythmic agent with multiple actions at ion channels. *Cardiovasc Drug Rev* 2006; 24: 101–15.
- 18 Li N, Yang L, Dai DZ, Wang QJ, Dai Y. Chiral separation of racemate CPU86017, an anti-arrhythmic agent, produces stereoisomers possessing favourable ion channel blockade and less alpha-adrenoceptor antagonism. *Clin Exp Pharmacol Physiol* 2008; 35: 643–50.
- 19 Li N, Dai DZ, Dai Y. CPU86017 and its isomers improve hypoxic pulmonary hypertension by attenuating increased ETA receptor expression and extracellular matrix accumulation. *Naunyn Schmiedeberg's Arch Pharmacol* 2008; 378: 541–52.
- 20 Nisbet RE, Graves AS, Kleinhenz DJ, Rupnow HL, Reed AL, Fan TH, *et al*. The role of NADPH oxidase in chronic intermittent hypoxia-induced pulmonary hypertension in mice. *Am J Respir Cell Mol Biol* 2009; 40: 601–9.
- 21 Ciamala C, Lin S, Liu WT, Dai DZ. Disposition and blood brain barrier of CPU-86017(P-choro-benzyl-tetra-hydroberberine) after iv and icv in mice. *J China Pharma Univ* 2002; 33: 226–30.
- 22 Yang TT, Guan L, Dai DZ, Zhang C. Comparison of protective effects and pharmacokinetics of CPU86017 and its chiral compounds (7S,13R)-CPU86017 on myocardial ischemia-reperfusion injury in rabbits. *Progr Pharmac Sci* 2007; 31: 26–31.
- 23 Lin S, Jia YP, Zeng S, Dai DZ. The pharmacokinetics of CPU86017 is determined in simply isolated rat microsome preparation. *Jiangsu Pharm and Clin Res* 2003; 11: 9–12.
- 24 Feng NP, Zhang ZX, An DK, Han XW, Huan WL, Wang GJ. Analysis of the metabolite of 7-(4-chlorobenzyl)-7,8,13,13a-tetrahydroberberine in rabbit. *Yao Xue Xue Bao* 2001; 36: 137–9.
- 25 Wedgwood S, Lakshminrusimha S, Farrow KN, Czech L, Gugino SF, Soares F, *et al*. Apocynin improves oxygenation and increases eNOS in persistent pulmonary hypertension of the newborn. *Am J Physiol Lung Cell Mol Physiol* 2012; 302: L616–26.
- 26 Kuo JJ, Chang HH, Tsai TH, Lee TY. Positive effect of curcumin on inflammation and mitochondrial dysfunction in obese mice with liver steatosis. *Int J Mol Med* 2012; 30: 673–9.
- 27 Verri M, Pastoris O, Dossena M, Aquilani R, Guerriero F, Cuzzoni G, *et al*. Mitochondrial alterations, oxidative stress and neuroinflammation in Alzheimer's disease. *Int J Immunopathol Pharmacol* 2012; 25: 345–53.
- 28 Azevedo LC. Mitochondrial dysfunction during sepsis. *Endocr Metab Immune Disord Drug Targets* 2010; 10: 214–23.
- 29 Vij AG, Kishore K, Dey J. Effect of intermittent hypobaric hypoxia on efficacy & clearance of drugs. *Indian J Med Res* 2012; 135: 211–6.
- 30 Wang Z, Zhang H, Xu X, Shi H, Yu X, Wang X, *et al*. bFGF inhibits ER stress induced by ischemic oxidative injury via activation of the PI3K/Akt and ERK1/2 pathways. *Toxicol Lett* 2012; 212: 137–46.
- 31 Fradette C, Batonga J, Teng S, Piquette-Miller M, du Souich P. Animal models of acute moderate hypoxia are associated with a down-regulation of CYP1A1, 1A2, 2B4, 2C5, and 2C16 and up-regulation of CYP3A6 and P-glycoprotein in liver. *Drug Metab Dispos* 2007; 35: 765–71.
- 32 Mantena SK, King AL, Andringa KK, Eccleston HB, Bailey SM. Mitochondrial dysfunction and oxidative stress in the pathogenesis of alcohol- and obesity-induced fatty liver diseases. *Free Radic Biol Med* 2008; 44: 1259–72.
- 33 Dhar SK, St Clair DK. Manganese superoxide dismutase regulation and cancer. *Free Radic Biol Med* 2012; 52: 2209–22.
- 34 Rahman MS, Thomas P. Effects of hypoxia exposure on hepatic cytochrome P450 1A (CYP1A) expression in Atlantic croaker: molecular mechanisms of CYP1A down-regulation. *PLoS One* 2012; 7: e40825.
- 35 Jurgens G, Christensen HR, Brosen K, Sonne J, Loft S, Olsen NV. Acute hypoxia and cytochrome P450-mediated hepatic drug metabolism in humans. *Clin Pharmacol Ther* 2002; 71: 214–20.
- 36 da Rosa DP, Forgiarini LF, Baronio D, Feijo CA, Martinez D, Marroni NP. Simulating sleep apnea by exposure to intermittent hypoxia induces inflammation in the lung and liver. *Mediators Inflamm* 2012; 2012: 879419.